ARTICLE

Involvement of cortical input to the rostromedial tegmental nucleus in aversion to foot shock

Elizabeth J. Glover [ID]1 ✉, E. Margaret Starr[1], Andres Gascon[1], Kacey Clayton-Stiglbauer[1], Christen L. Amegashie[1], Alyson H. Selchick[2], Dylan T. Vaughan[2], Wesley N. Wayman[2], John J. Woodward [ID]2 and L. Judson Chandler[2]

The rostromedial tegmental nucleus (RMTg) encodes negative reward prediction error (RPE) and plays an important role in guiding behavioral responding to aversive stimuli. Previous research has focused on regulation of RMTg activity by the lateral habenula despite studies revealing RMTg afferents from other regions including the frontal cortex. The current study provides a detailed anatomical and functional analysis of cortical input to the RMTg of male rats. Retrograde tracing uncovered dense cortical input to the RMTg spanning the medial prefrontal cortex, the orbitofrontal cortex and anterior insular cortex. Afferents were most dense in the dorsomedial subregion of the PFC (dmPFC), an area that is also implicated in both RPE signaling and aversive responding. RMTg-projecting dmPFC neurons originate in layer V, are glutamatergic, and collateralize to select brain regions. In-situ mRNA hybridization revealed that neurons in this circuit are predominantly D1 receptor-expressing with a high degree of D2 receptor colocalization. Consistent with cFos induction in this neural circuit during exposure to foot shock and shock-predictive cues, optogenetic stimulation of dmPFC terminals in the RMTg drove avoidance. Lastly, acute slice electrophysiology and morphological studies revealed that exposure to repeated foot shock resulted in significant physiological and structural changes consistent with a loss of top-down modulation of RMTg-mediated signaling. Altogether, these data reveal the presence of a prominent cortico-subcortical projection involved in adaptive behavioral responding to aversive stimuli such as foot shock and provide a foundation for future work aimed at exploring alterations in circuit function in diseases characterized by deficits in cognitive control over reward and aversion.

INTRODUCTION

The rostromedial tegmental nucleus (RMTg), also referred to as the tail of the VTA, is a cluster of GABAergic neurons located immediately posterior to the VTA [1, 2]. The RMTg receives dense input from the lateral habenula (LHb) and exerts inhibitory control over aminergic and cholinergic midbrain nuclei including dopamine neurons of the VTA. RMTg activity increases in response to aversive stimuli [3, 4] and loss of RMTg function enhances active (e.g., escape) while reducing passive (e.g., freezing) responding in tests measuring fear and learned helplessness [3, 5].

The prefrontal cortex (PFC) integrates incoming multisensory information with previous experience to provide top-down inhibitory control over behavior and guide goal-directed responding. Interestingly, subregions spanning the dorsomedial PFC (dmPFC), which includes the anterior cingulate cortex (ACC) and prelimbic (PL) PFC, exhibit a number of functional similarities with the RMTg. For example, similar to the RMTg, neuronal activity in the PL PFC increases during exposure to aversive stimuli [6] and loss of PL function reduces passive fear responding [7]. In addition, activity in both the dmPFC [8] and RMTg [9] has been implicated in signaling reward prediction error (RPE).

Initial anatomical characterizations of the RMTg revealed the presence of cortical afferents to the RMTg, including some arising from the frontal cortex [1, 2]. However, the anatomy and function of these inputs have not been well-characterized, as much of the research aimed at investigating the role of RMTg-associated neural circuits in aversive signaling has focused on the LHb-RMTg-VTA projection. The present study addressed this gap in our knowledge by anatomically defining cortical inputs to the RMTg and used optogenetics, electrophysiology, and imaging techniques to determine their functional role in aversive signaling. Our results demonstrate that cortical afferents to the RMTg arise from functionally distinct regions of the medial prefrontal, orbitofrontal, and insular cortices. Because the dmPFC and RMTg share functional similarities, we hypothesized that RMTg-projecting dmPFC neurons play a role in top-down control over RMTg-mediated aversive signaling. Consistent with this hypothesis, our results demonstrate that dmPFC input to the RMTg drives avoidance behavior and that this neural circuit undergoes significant structural and functional changes following exposure to repeated foot shock.

MATERIALS AND METHODS

Animals

For all experiments, adult male Long-Evans rats (P60 upon arrival, Envigo Laboratories, Indianapolis, IN) were individually housed in standard

[1]Center for Alcohol Research in Epigenetics, Department of Psychiatry, University of Illinois at Chicago, Chicago, IL, USA. [2]Department of Neuroscience, Medical University of South Carolina, Charleston, SC, USA. ✉email: ejglover@uic.edu

polycarbonate cages. The vivarium was maintained on a 12:12 reverse light-dark cycle with lights off at 09:00. Rats were habituated to the vivarium for at least one week before beginning experiments. All rats were provided with Teklad 2918 (Envigo) standard chow and water *ad libitum*. Rats underwent stereotaxic surgery to enable selective labeling of RMTg-projecting cortical neurons as described in the Supplementary Methods. All experiments were approved by the Institutional Animal Care and Use Committees at the Medical University of South Carolina and University of Illinois at Chicago and adhered to the guidelines put forth by the NIH [10].

Anatomical analyses
Cell density, cell type, and extent of collateralization were analyzed by quantifying standard immunolabeling using ImageJ. In-situ hybridization was performed using RNAScope and analyzed in Imaris. See Supplementary Methods for additional details.

Functional analyses
Real-time place preference during optical stimulation was performed using previously published procedures [11]. cFos induction following exposure to aversive stimuli was performed using methods identical to those described in Jhou et al. [3]. Whole-cell patch-clamp slice electrophysiology was performed using previously published methods [12]. Dendritic spine density analysis was performed in Imaris using previously published methods [13]. See Supplementary Methods for additional details.

Statistical analysis
The total number of cells analyzed as well as average number of cells analyzed per rat for each anatomical assessment is summarized in Table S2. Student's *t*-test and analysis of variance (ANOVA) were performed to analyze functional data, and a Greenhouse-Geisser correction was performed on data that lacked sphericity. All statistical analyses were performed using GraphPad Prism 8.0. Data are presented as mean ± SEM, and effects were considered statistically significant at $p \leq 0.05$.

RESULTS
Cortical input to the RMTg is dense and collateralizes selectively throughout the brain
While initial reports describing the RMTg indicated the presence of cortical efferents, the magnitude of this input and subregional distribution was unclear. To more clearly define these inputs, RMTg-projecting cell bodies were quantified in rat brains injected with the retrograde tracer cholera toxin B (CtB). Visual inspection of slices double stained for CtB and the neuronal marker, NeuN, revealed the presence of dense input spanning the medial PFC (mPFC) and orbitofrontal cortex (OFC), in addition to relatively low but consistent labeling in the anterior insular cortex (AIC) in agreement with previous reports (Fig. 1) [1, 2]. The majority of CtB-labeled cell bodies were primarily found in layer V (Fig. 1C). Quantification of CtB+ neurons relative to NeuN+ neurons in layer V of the mPFC revealed relatively uniform densities of RMTg-projecting neurons across the rostrocaudal extent of ACC (3.96 ± 0.28%), PL (8.59 ± 0.45%), and IL (7.95 ± 0.77%) subregions (Fig. 1D). In contrast, the density of RMTg-projecting dorsopeduncular (DP) mPFC neurons increased substantially at more caudal levels relative to rostral DP mPFC (13.02 ± 2.91%).

To assess the difference in density between ipsilateral and contralateral hemispheres, we compared the density of layer V RMTg-projecting neurons across hemispheres in the PL region of the PFC. As expected, cell density in the contralateral hemisphere was less than that of the ipsilateral projection (4.07 ± 0.20%) (Fig. 1E). A two-way RM ANOVA comparing cell density between hemispheres across the rostrocaudal extent of the PL confirmed that significantly fewer RMTg-projecting cells were observed in the contralateral compared to ipsilateral hemisphere regardless of rostrocaudal level [main effect of hemisphere: $F_{(1,16)} = 45.09$, $p < 0.0001$].

The density of CtB-labeled neurons was relatively similar across rostral subregions of the OFC, but diverged caudally (Fig. 1F).

On average, the density of CtB labeling was greatest but somewhat variable in the medial orbital (MO) cortex (8.01 ± 1.32%), while labeling in the dorsolateral orbital (DLO) cortex was lower and less variable (5.48 ± 0.62%). In the ventro-orbital (VO) and latero-orbital (LO) cortex, the density of CtB labeling varied substantially along the rostrocaudal axis. In the VO, a U-shaped pattern was observed with relatively dense labeling at the rostral (9.18 ± 1.43%) and caudal extents of the region (7.03 ± 1.87%) that far exceeded the degree of labeling observed at the mid-point through the rostrocaudal axis (4.35 ± 0.98%). By contrast, RMTg-projecting neurons arising from the LO cortex are most dense at the rostral tip of the region (7.45 ± 1.43%) with very little CtB labeling in the most caudal area (1.05 ± 0.73%).

Although substantially less dense than projections arising from the mPFC and OFC, CtB labeling of projections to the RMTg was consistently observed in subregions of the AIC (Fig. 1G). Within this region, the density of labeling was greatest in the agranular cortex with approximately 4.5% of layer V neurons in dorsal (AID) and ventral (AIV) subregions projecting to the RMTg (AID: 4.77 ± 0.65%; AIV: 4.49 ± 0.72%). By contrast, CtB labeling was approximately half of this amount in the dysgranular (DI; 2.8 ± 0.76%) and granular (GI; 2.43 ± 0.84%) AIC.

To examine the extent of collateralization of RMTg-projecting dmPFC neurons, this projection was selectively filled with green fluorescent protein using an intersectional, dual-virus approach in four rats (Fig. 1H). Labeling was absent in one rat that was, therefore, excluded from analysis. In the remaining three rats, labeling was targeted to the dmPFC, was restricted to the injected hemisphere, and was not apparent in cell bodies outside of the dmPFC indicating successful isolation of the dmPFC-RMTg circuit (Fig. 1I). Dense punctate labeling, traditionally interpreted to reflect synaptic terminals [14], was evident in a number of subcortical regions. Quantification of staining density revealed dense collateralization in select subcortical regions (Fig. 1H–K; see Supplementary results for additional details of this analysis).

RMTg-projecting dmPFC neurons are glutamatergic and co-express D1 and D2 mRNA
While layer V cortical efferents are typically considered to be excitatory in nature, recent work has revealed the presence of long-range GABAergic projection neurons arising from cortical regions [15–17]. To determine whether RMTg-projecting cortical neurons were glutamatergic or GABAergic, a subset of CtB-labeled slices adjacent to those used in the cell density analysis were immunostained for either CaMKIIα or GAD67. As shown in Fig. 2A–D, CtB-labeled neurons were predominantly CaMKIIα+, and virtually no overlap in expression was observed between CtB and the GABAergic marker, GAD67. These data indicate that RMTg-projecting cortical neurons are glutamatergic projection neurons.

Both D1 and D2 dopamine receptors in the PFC are known to play important roles in regulating behavioral flexibility and decision-making [18]. Dopamine receptor-mediated signaling in the mPFC is also implicated in defensive behavior and aversion learning [19–22]. In addition, several studies suggest that D1- and D2-expressing neurons in the mPFC may represent anatomically and functionally distinct cell populations [e.g., [23]]. These data led us to consider whether RMTg-projecting dmPFC neurons exhibited a unique dopamine receptor expression profile that contributed to the regulation of RMTg-mediated aversive signaling. To investigate this, we measured the D1/D2 expression profile of RMTg-projecting dmPFC neurons by combining fluorescent retrograde tracing with in-situ hybridization via RNAScope for D1 and D2 receptor mRNA. As shown in Fig. 2E–H, classification of retrobead-labeled cells by dopamine receptor mRNA expression revealed that a majority of RMTg-projecting dmPFC neurons express D1 receptors (87%), with a substantial proportion also
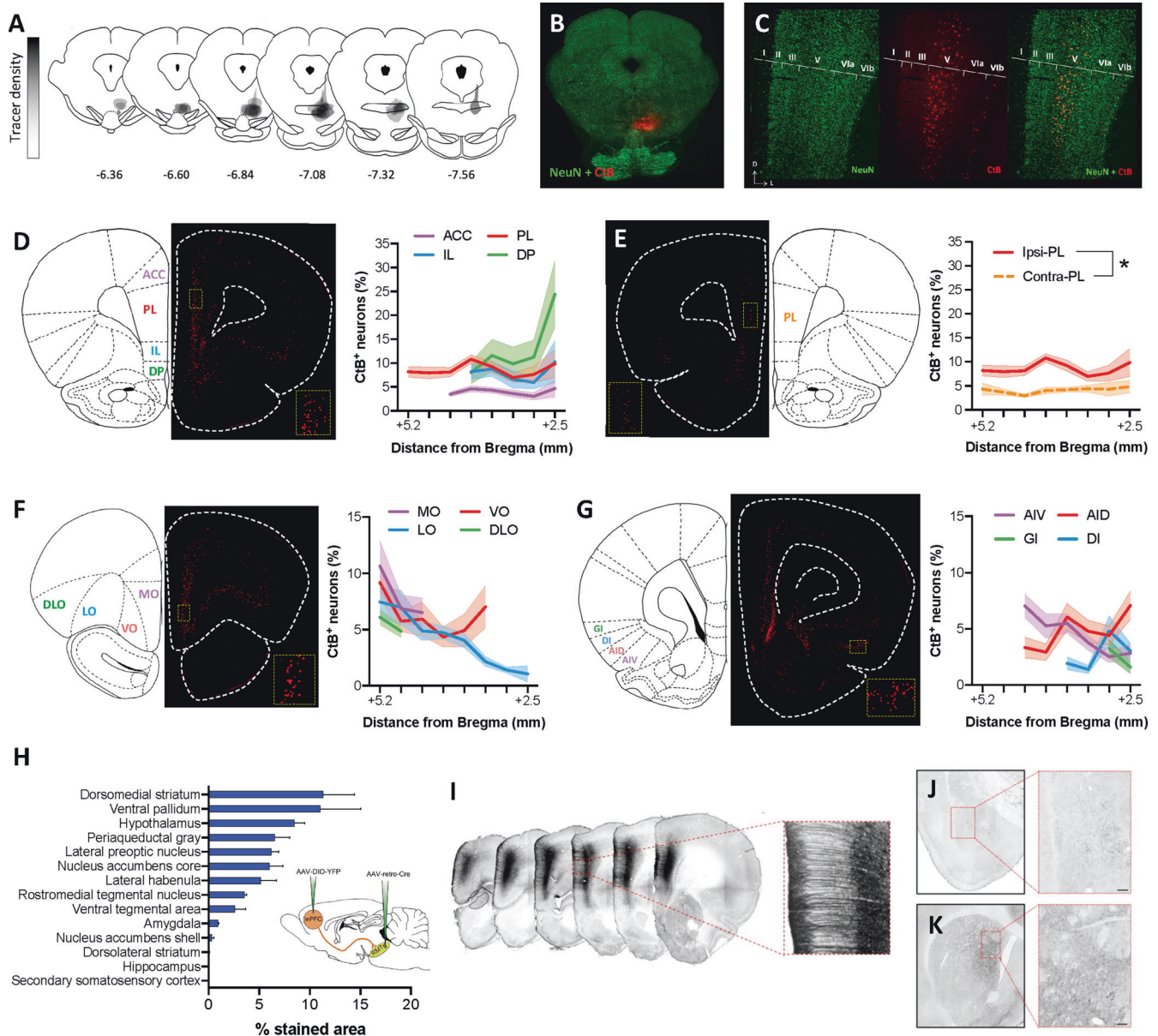
Fig. 1 Anatomical characterization of cortical inputs to the RMTg. A Map of cholera toxin B (CtB) retrograde tracer injection sites for all animals included in quantification. **B** Representative injection site image. **C** Representative high magnification image showing that inputs to the RMTg arise primarily from layer V of the mPFC. **D** The percent of CtB+ neurons relative to all layer V NeuN+ neurons is relatively consistent across ACC, PL, and IL subregions of the mPFC whereas the density of RMTg-projecting DP mPFC neurons increases substantially at more caudal levels. **E** Contralateral cortical afferents are substantially less dense than ipsilateral inputs as exemplified by a comparison of RMTg-projecting PL mPFC neurons in both hemispheres. **F** The density of layer V OFC neurons projecting to the RMTg is similar to that observed in the mPFC with LO inputs diminishing at more caudal levels. **G** CtB labeling is consistently observed in the AIC, albeit to a lesser degree than that observed in mPFC and OFC. **H** Quantification of punctate labeling indicative of collateral input from ROIs placed within each brain region in rats prepared using an intersectional dual-virus approach (inset) to fill RMTg-projecting dmPFC neurons with yellow fluorescent protein (YFP). **I** Representative images showing RMTg-projecting dmPFC neurons filled with YFP following amplification using standard immunohistochemistry. **J** Representative YFP staining in the amygdala shows relatively sparse collateralization of RMTg-projecting dmPFC neurons in the basolateral nucleus. **K** Representative YFP staining in the striatum shows dense collateralization in the dorsomedial but not dorsolateral striatum. Scale bar = 100 μm. ACC anterior cingulate cortex, AID dorsal agranular insular cortex, AIV ventral agranular insular cortex, DI dysgranular insular cortex, DLO dorsolateral orbitofrontal cortex, DP dorsopeduncular cortex, GI granular insular cortex, IL infralimbic cortex, LO lateral orbitofrontal cortex, MO medial orbitofrontal cortex, PL prelimbic cortex, VO ventral orbitofrontal cortex.

expressing D2 receptors (59%). Only a small proportion of retrobead labeled neurons expressed D2 mRNA in the absence of D1 mRNA (5%), and approximately 8% of the bead labeled neurons lacked mRNA for either receptor. Taken together, these observations reveal that a large population of dmPFC neurons that project to the RMTg are glutamatergic neurons and co-express D1 and D2 receptor mRNA.

Selective stimulation of RMTg-projecting dmPFC neurons drives avoidance behavior

To investigate whether dmPFC inputs to the RMTg play a significant role in aversive signaling, in-vivo optogenetics was used to measure real-time place preference in response to activation of this neural circuit. To achieve this, rats were injected with the excitatory opsin, channelrhodopsin (ChR2), into the
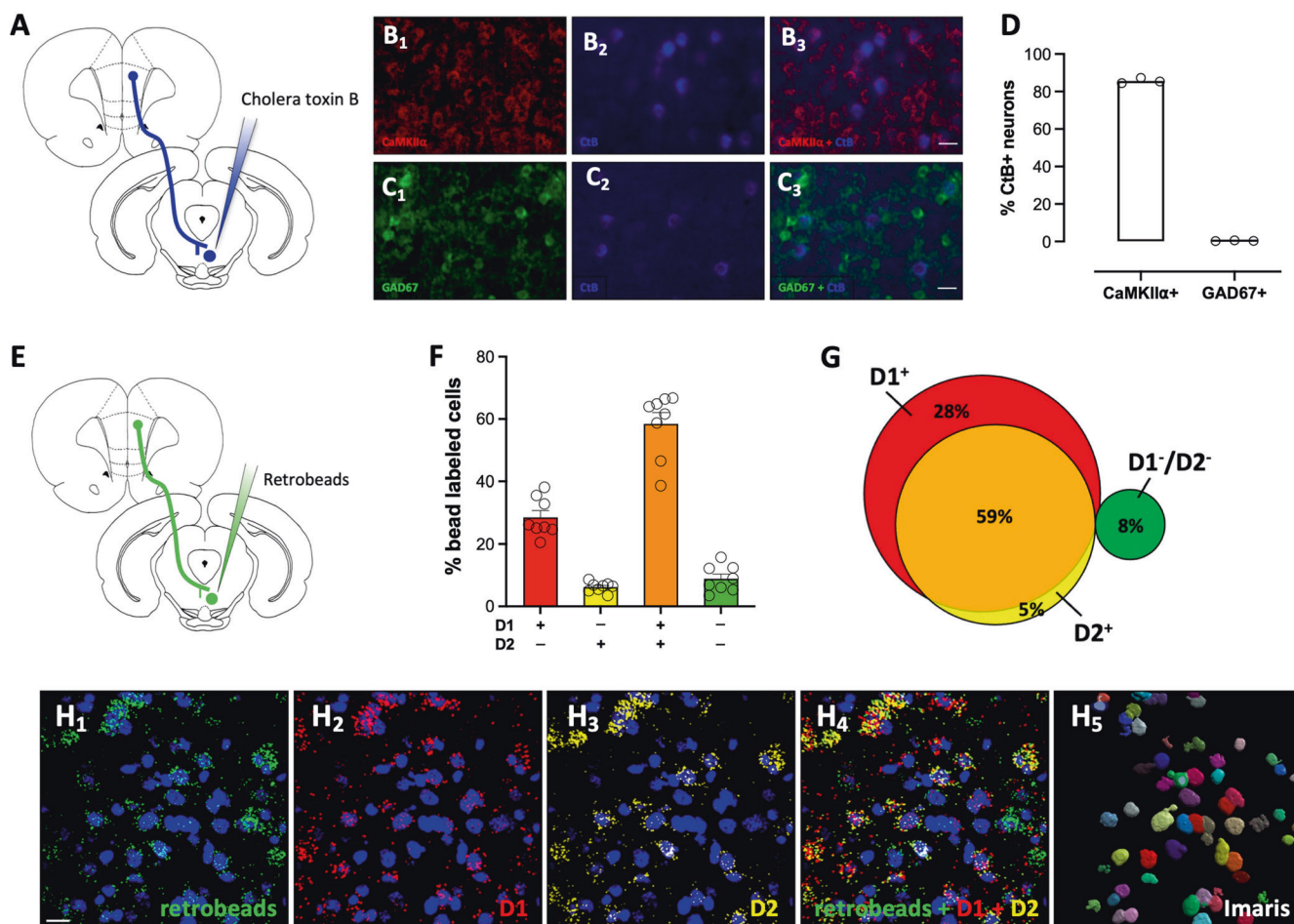
Fig. 2 RMTg-projecting dmPFC neurons express glutamatergic markers and are positive for D1 and D2 receptor mRNA. A Rats were injected with the retrograde tracer, cholera toxin B (CtB), into the RMTg and slices prepared for dual immunofluorescence. Representative dmPFC images co-labeled for the **B$_{1-3}$** glutamatergic marker CaMKIIα (red) and CtB (blue) and the **C$_{1-3}$** GABAergic marker GAD67 (green) and CtB (blue). Scale bar = 25 μm. **D** Quantification of co-labeling reveals that RMTg-projecting neurons are CaMKIIα$^+$. **E** For in-situ hybridization, fluorescent retrobeads were injected into the RMTg and slices processed using RNAScope. **F, G** Quantification of D1 and D2 mRNA labeling in retrobead+ cells revealed that most RMTg-projecting dmPFC neurons express transcript for both D1 and D2 receptors. **H$_{1-5}$** Representative dmPFC images co-labeled with retrobeads (green), D1 mRNA (red), and D2 mRNA (yellow), as well as an image of Imaris rendered 3D soma, which was used for defining neuronal labeling of the bead and mRNA transcripts. Scale bar = 20 μm.

dmPFC (Fig. 3A) or LHb and optic fibers implanted to stimulate terminals in either the RMTg or VTA (Figs. S1 and 3B–D). Testing on day 1 revealed that stimulation of dmPFC terminals in the RMTg resulted in significant avoidance of the light-paired compartment relative to chance (Fig. 3B). This effect was replicated during testing on day 2 when the light-paired compartment was reversed [one-way ANOVA test 1 × test 2 × chance: $F(1.95, 7.75) = 22.74$; $p = 0.0006$]. The magnitude of this avoidance was similar to that observed during stimulation of LHb terminals in the RMTg (Fig. 3C), which was also significantly lower than chance [one-way ANOVA test 1 × test 2 × chance: $F(1.59, 7.95) = 9.60$; $p = 0.0095$]. In contrast, stimulation of dmPFC terminals in the neighboring VTA resulted in neither preference nor avoidance of the light-paired compartment (Fig. 3D) on either day 1 or day 2 [one-way ANOVA test 1 × test 2 × chance: $F(1.04, 3.11) = 0.095$; $p = 0.7866$]. Direct comparison of the effect of each circuit manipulation on real-time place preference revealed that stimulation of either dmPFC or LHb inputs to the RMTg drove avoidance behavior that was significantly different from stimulation of dmPFC inputs to the VTA (Fig. 3E) [one-way ANOVA: $F(2, 12) = 7.30$, $p = 0.0084$]. Altogether, these data indicate that activation of dmPFC inputs to the RMTg provides an aversive signal to promote avoidance behavior.

RMTg-projecting mPFC neurons are activated following exposure to foot shock and tones predictive of foot shock

While optogenetic stimulation of dmPFC-RMTg neurons can facilitate avoidance, it is still unknown whether neurons in this circuit are activated during responding to aversive stimuli such as foot shock. To explore this possibility, rats in which CtB had been injected into the RMTg were euthanized 90 min after exposure to either neutral or aversive stimuli (Fig. 4A). Two groups of rats were exposed to a series of tones and foot shocks. In one group, tones were predictive of shock as in a standard fear conditioning paradigm. In the other group, rats were exposed to the same number of tones and shocks but in an unpaired manner such that tones were not predictive of shock. As expected, rats in the Shock-paired tone group exhibited significantly greater freezing in response to tone presentation on test day than rats in the Shock-unpaired group (t-test; $p = 0.0005$; Fig. 4B). Behavioral data was not collected on the two remaining groups of rats exposed to either the neutral testing context or a series of foot shocks (without tone presentation). A one-way ANOVA comparing the magnitude of cFos expression in CtB-labeled neurons in the mPFC revealed a significant effect of treatment condition on cFos induction (Fig. 4C, D) [$F(3, 32) = 11.00$, $p < 0.0001$]. Tukey's post-hoc comparisons revealed that cFos expression was significantly
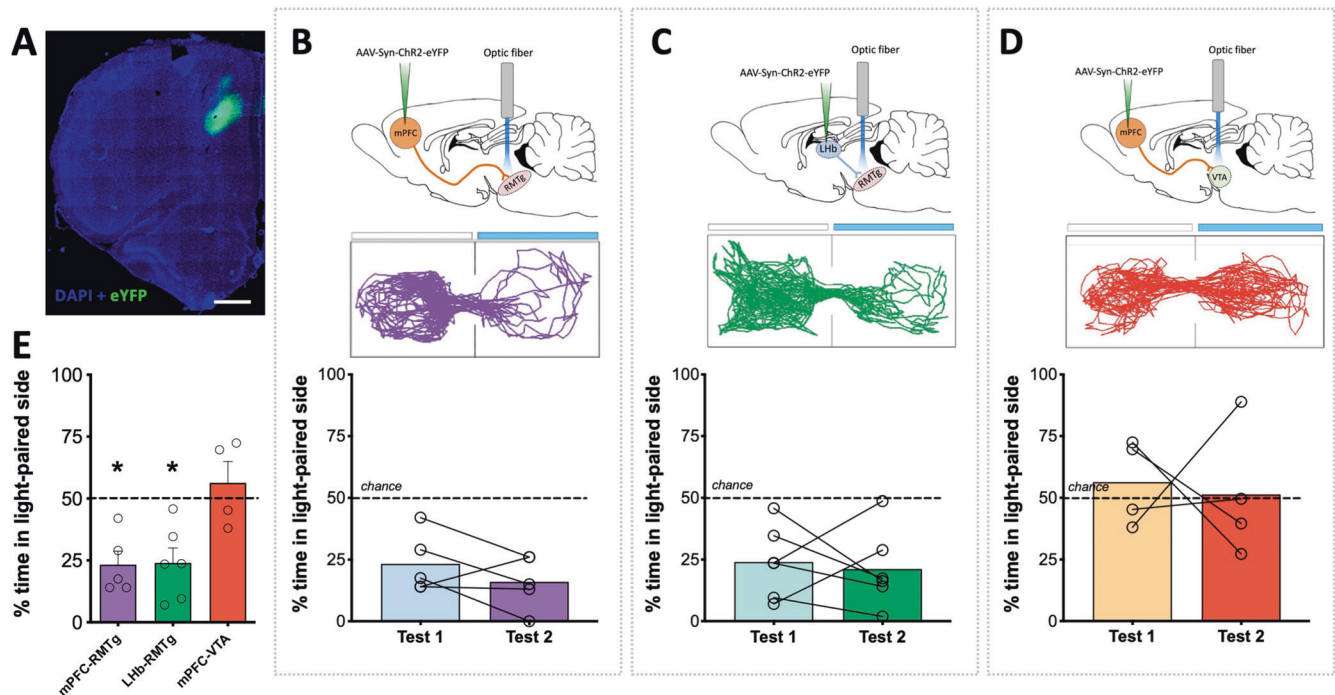
Fig. 3 Optogenetic stimulation of RMTg-projecting dmPFC terminals drives avoidance. A Representative ChR2 expression in dmPFC. **B** Rats spend significantly less time relative to chance in the light-paired side of a two-compartment chamber during initial testing (test 1) and when the light-paired compartment is reversed (test 2) when light delivery results in stimulation of dmPFC terminals in the RMTg. **C** A similar degree of avoidance of the light-paired chamber is observed upon stimulation of lateral habenula inputs to the RMTg. **D** Unlike stimulation of dmPFC terminals in the RMTg, stimulation of dmPFC terminals in the VTA fails to produce either preference for or avoidance of the light-paired compartment. **E** Direct comparison of circuit manipulations reveals significant avoidance when stimulating inputs to the RMTg relative to the VTA. Light-paired side indicated by blue bar in representative maps above each dataset. *$p \leq 0.01$, scale bar = 1000 μm.

greater in RMTg-projecting mPFC neurons of rats that were exposed to either foot shocks or tones predictive of shocks relative to rats exposed to the neutral testing context (shock: $p < 0.0001$; shock-paired tone: $p = 0.006$). The magnitude of cFos expression in CtB-labeled mPFC neurons in shock-exposed rats was also significantly greater than was observed in rats exposed to tones that were unpaired with shocks ($p = 0.004$). In combination with results from the real-time place preference testing, these data suggest that RMTg-projecting mPFC neurons are activated in response to conditioned and unconditioned aversive stimuli and may play a role in regulating the behavioral response to such stimuli.

Functional and structural changes in RMTg-projecting dmPFC neurons following exposure to repeated foot shock

We next investigated the potential impact that exposure to repeated foot shock has on the excitability of dmPFC neurons that project to the RMTg (Fig. 5). A two-way repeated measures ANOVA of spiking measured during whole-cell patch-clamp recordings from RMTg-projecting dmPFC neurons revealed a significant interaction between current step and stimulus exposure [$F(15,315) = 22.08$, $p < 0.0001$] such that spike frequency was significantly reduced in rats exposed to the same foot shock procedure that induced significant cFos expression relative to Context controls (Sidak correction; all p values ≤ 0.03; Fig. 5C, D). Action potential and membrane parameters were analyzed (Fig. 5E–K) and showed that the reduction in spiking was accompanied by a significantly higher rheobase (t-test; $p < 0.0001$), significantly lower membrane resistance (t-test; $p < 0.0001$), and higher membrane capacitance (t-test; $p < 0.0434$) in Shock-exposed rats compared to context controls. No significant difference in action potential threshold was observed between groups (t-test; $p = 0.1555$). Action potential

duration and amplitude were significantly different between groups with Shock-exposed rats exhibiting action potentials of greater amplitude (t-test; $p = 0.0232$) and shorter duration (t-test; $p = 0.0002$) than Context-exposed rats. No significant difference in action potential after-hyperpolarization was observed between groups (t-test; $p = 0.2625$). Overall, these data are indicative of decreased intrinsic excitability in RMTg-projecting dmPFC neurons following exposure to foot shock.

To examine the impact of exposure to aversive stimuli on structural plasticity, we next quantified dendritic spine density and morphology in RMTg-projecting dmPFC neurons labeled using an intersectional virally-mediated approach (Fig. 5L) in rats exposed to either foot shock or a neutral context. T-tests were used to analyze differences in dendrite diameter and volume as well as dendritic spine density collapsed across spine class. Two-way ANOVAs were used to analyze spine density and morphology by spine class between groups. No significant differences in dendrite diameter, volume or overall spine density were observed between Context- and Shock-exposed rats (p values > 0.50; Table S1). Analysis of spine density revealed a main effect of spine class [$F(3,40) = 53.37$, $p < 0.0001$] but no main effect of stimulus exposure [$F(1,40) = 0.075$, $p = 0.7856$] or interaction between the two factors [$F(3,40) = 1.34$, $p = 0.2756$]. Tukey corrected post-hoc comparisons of the main effect of spine class revealed that both Context- and Shock-exposed rats had a significantly greater density of mushroom-shaped spines relative to all other spine classes (all p values < 0.0001; Fig. 5L–N). The majority of measures indicative of spine morphology were not affected by shock exposure (Table S1). One notable exception was spine neck diameter, which was significantly greater in Shock-exposed rats across all spine classes compared to Context-exposed rats (Table S1; Fig. 5O). Differences in spine neck length were also observed between Context- and Shock-exposed rats (Table S1; Fig. 5P).
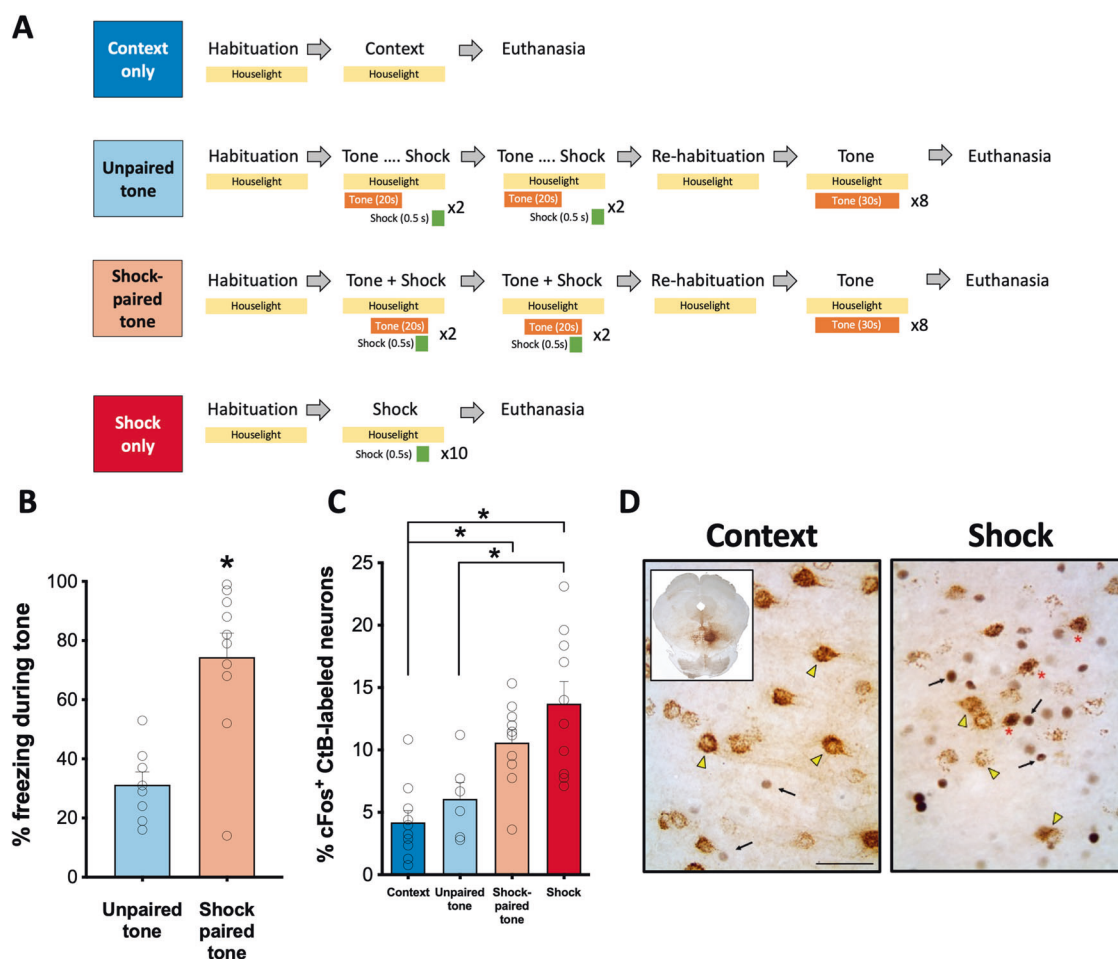
Fig. 4 cFos induction in RMTg-projecting dmPFC neurons following exposure to aversive stimuli. A Experimental procedures. **B** Rats that had tone paired with foot shock delivery displayed significantly more freezing behavior in response to tone presentation than rats that were exposed to the same number of tone-shock presentations but in an unpaired manner. **C** Significantly greater cFos expression was observed in RMTg-projecting dmPFC neurons (CtB+) following exposure to either a series of foot shocks or a tone predictive of foot shock relative to a neutral tone or the testing context alone. **D** Representative images of CtB and cFos labeling in the dmPFC of a context-exposed rat and a rat exposed to foot shock. Representative CtB$^+$/cFos$^-$ neurons are indicated with a yellow arrowhead; Representative CtB$^-$/cFos$^+$ neurons are indicated with a black arrow; Representative CtB$^+$/cFos$^+$ neurons are indicated by a red asterisk. Inset shows representative injection site in RMTg. Scale bar = 200 μm.

Quantification of D1, D2, and cFos mRNA expression was also performed in Shock- and Context-exposed rats using the same tissue analyzed in Fig. 2. While cFos mRNA was significantly increased in Shock-exposed rats relative to Context controls (two-way ANOVA main effect of treatment: $F(1,12) = 4.72$, $p = 0.0505$), cFos induction was not specific to a unique dopamine receptor-expressing population of dmPFC-RMTg neurons and exposure to repeated foot shocks had no effect on D1 or D2 mRNA levels (Figs. S2 and S3; see Supplement for additional details).

DISCUSSION

The findings of the present study revealed the presence of dense cortical input to the RMTg spanning the mPFC, OFC and AIC. Analysis of RMTg afferents arising in the dmPFC revealed that these cortical projection neurons are glutamatergic, with the majority expressing mRNA for both D1 and D2 receptors. Our results further reveal that RMTg-projecting dmPFC neurons send collaterals to other brain regions that are critically involved in regulating motivated behavior and flexible decision-making. Stimulation of dmPFC terminals in the RMTg drove avoidance, consistent with the observation that exposure to foot shock or a shock-predictive cue induced cFos expression in dmPFC-RMTg

neurons. Finally, we showed that repeated exposure to foot shock decreased the intrinsic excitability of these neurons and induced subtle alterations in spine structure. Collectively, the results of this study suggest that dmPFC neurons play an important role in governing RMTg-mediated aversive responding. However, it should be noted that the current study was limited to findings in male rats. Given that significant sex differences exist with respect to nociception [24], risk assessment [25], and threat responding [26], it will be important that future studies expand upon the present observations to define potential sex differences in dmPFC-RMTg function.

As anatomical density can determine the influence of a circuit over behavior, our data suggest that mPFC inputs to the RMTg are likely to play an equally important role in guiding adaptive responding to environmental stimuli as do other cortico-subcortical circuits. For example, prior quantitative analysis of cortico-subcortical projection density in the mPFC reported that ~8% of layer V PL and IL mPFC neurons project to the amygdala and ~18% project to the ventral striatum [27]. In contrast, only ~1–5% of layer V PL and IL neurons project to the raphe and periaqueductal gray. Importantly, each of these projections – even those that are relatively sparse – have been implicated in regulating crucial aspects of motivated behavior [e.g., [28–30]].
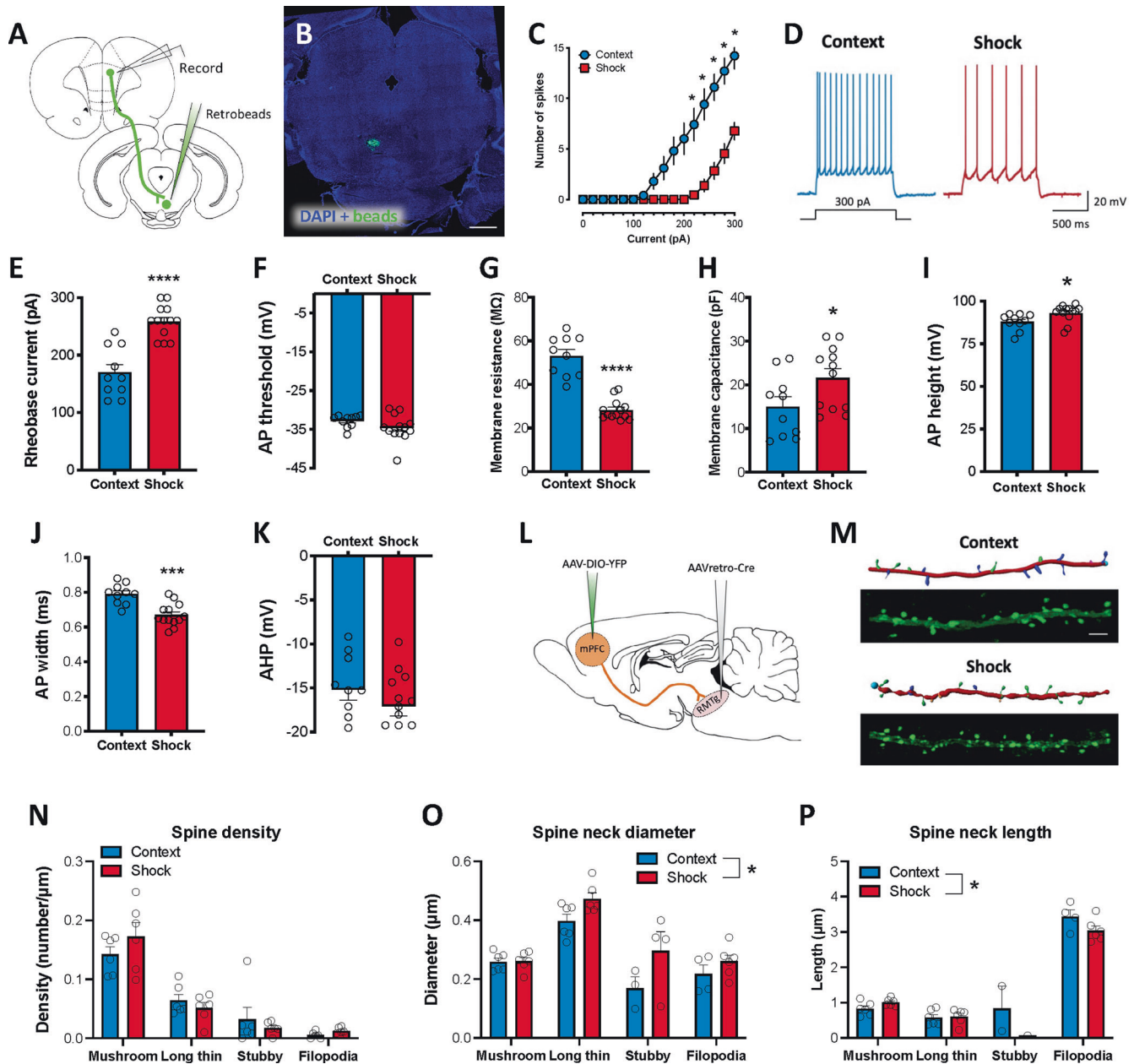
Fig. 5 Physiological and structural neuroadaptations in RMTg-projecting dmPFC neurons following exposure to foot shock. A For ex-vivo electrophysiology experiments, rats were injected with retrobeads into the RMTg. **B** Representative retrobead injection site in the RMTg. Scale bar = 1000 μm. **C** Significantly fewer spikes were observed in Shock-exposed rats relative to controls in current clamp recordings of retrobead-labeled dmPFC neurons. **D** Representative traces from a control and Shock-exposed rat. Decreased spiking was associated with a significant increase in **E** rheobase, **H** membrane capacitance, and **I** action potential height as well as a significant decrease in **G** membrane resistance and **J** action potential half-width. No significant difference was observed in **F** action potential threshold or **K** after hyperpolarization. **L** For structural analyses, an intersectional dual-virus approach was used to fill RMTg-projecting dmPFC neurons with yellow fluorescent protein (YFP). **M** Representative YFP-filled primary apical dendrites in the dmPFC and accompanying Imaris renderings for Context- and Shock-exposed rats. Scale bar = 5 μm. **N** Spine density did not differ between groups regardless of subclass. However, Shock-exposed rats exhibited significantly greater spine neck diameter **O** and shorter spine length **P** across all subtypes (main effect of shock) relative to rats exposed to the neutral testing context. *$p \leq 0.05$.

By comparison, our investigation revealed that ~10% of layer V dmPFC neurons project to the RMTg and that this relatively dense projection also regulates motivated behavior.

Using an intersectional, virally-mediated approach, we observed dense collateralization of RMTg-projecting dmPFC neurons to a number of regions that have also been shown to play a critical role modulating motivated behavior. While the extent of collateralization of the dmPFC-RMTg circuit may be somewhat surprising, this frequently underappreciated aspect of neuronal structure is actually quite common. Indeed, recent methodological advancements have enabled researchers to map the extent of a single neuronal projection throughout the brain and demonstrate that collateralization is often widespread [31–33]. The extensive collateralization of the dmPFC-RMTg projection is consistent with this circuit being part of a highly interconnected network of brain areas involved in modulating various aspects of motivated behavior, including responding to aversive stimuli. Collateralization of the dmPFC-RMTg projection was most dense in the

dorsomedial striatum. This is particularly interesting as previous studies have established an important role for dmPFC afferents to the dorsomedial striatum in guiding goal-directed behavior [34] including avoidance [35]. While terminal density in the RMTg was relatively low in the present study by comparison to other regions, it is known that collaterals are often comprised of very thin branches [36]. Therefore, the density measurement we obtained (i.e., percent area stained) may not provide a full picture of the extent of collateralization of this projection. It is also unclear from our data whether the observed collateralization is indicative of dense arborization of a few dmPFC neurons, or of a large number of dmPFC cells each providing relatively weak collateral input to a given region. Recent work reporting very little overlap in cell body labeling between NAc- and RMTg-projecting mPFC neurons using dual retrograde tracer approach [37] suggests that the former may be the more likely scenario. The design of the present study does not allow for the identification of potential dmPFC-RMTg subpopulations, which could exhibit distinct sets of collaterals (e.g., ventral vs dorsal collateral streams) as has been shown in other studies [33]. Moreover, the current experimental approach did not allow us to discriminate between the possible presence of both functional and non-functional synaptic contacts. Additional experiments using multiple retrograde tracers to examine overlap in dmPFC cell body labeling and specific markers of active synaptic contacts will be essential to understand the potential functional implications of synergistic neurotransmission in regions receiving collateral input.

Dopamine signaling via D1 and D2 receptors in the mPFC is known to play an important role in modulating adaptive learning and decision-making. In the present study, we observed that RMTg-projecting dmPFC neurons are glutamatergic and predominantly express D1 dopamine receptor mRNA, with a significant proportion also co-expressing mRNA for D2 receptors. These findings agree with existing data showing that D1 receptor expression is greater than that of D2 in the mPFC [38]. While D1 and D2 receptor-expressing neurons are often thought of as discrete cell populations, a number of studies have observed colocalization of both receptors, particularly in layer V of the mPFC [23, 38, 39]. Recent work highlights the importance of dopaminergic regulation of cortical control in aversive signaling [40, 41]. Of particular interest is data suggesting that dopamine signaling alters mPFC responses to aversive stimuli by altering the signal-to-noise ratio of incoming sensory inputs [40]. Whether this dopaminergic modulation is circuit- or cell-type specific is not well-understood. Nevertheless, a rich literature demonstrates that D1 and D2 receptors regulate behavioral flexibility in complex ways in the mPFC [42] likely by altering neuronal excitability and synaptic transmission. Moreover, D1 and D2 receptor-mediated dmPFC signaling is differentially disrupted in some models of neuropsychiatric illness [43, 44], presenting the possibility that dopamine-mediated dysregulation of dmPFC-RMTg circuitry plays a role in maladaptive behaviors characteristic of such illnesses.

The current study also demonstrated that stimulation of dmPFC terminals in the RMTg facilitates real-time place avoidance. Importantly, this effect was similar in magnitude to what we and others [11] observed using the same light-delivery parameters to stimulate LHb terminals in the RMTg. While this approach allows for direct comparison between the effect observed in the current study and previous work, it should be noted that it is unlikely that either dmPFC or LHb afferents fire at 60 Hz—even in response to salient environmental stimuli [see [45, 46] for example]. Our data revealing significant cFos induction in RMTg-projecting dmPFC neurons during exposure to repeated shock or a shock-predictive cue complement the real-time place preference data by demonstrating that not only can stimulation of this circuit facilitate avoidance but that activity within this circuit is indeed recruited during responding to an aversive stimulus such as foot shock. Importantly, the relatively simple behavioral assays

employed in the current study are not designed to disambiguate complex aspects of defensive responding. Thus, the use of more sophisticated approaches to determine whether dmPFC-RMTg neuron activity regulates both active and passive avoidance as well as other innate defensive responses is an important area for future investigation. This is particularly true in light of previous data showing that loss of RMTg function shifts responding to aversive stimuli from a passive to active defense strategy [3].

Data from the present study is unable to determine whether RMTg-projecting dmPFC neurons are involved in aversion learning or if they simply encode general information regarding stimulus valence. The fact that cFos induction was significantly greater in rats exposed to either foot shock or a shock-predictive cue compared to context-exposed controls suggests that this circuit is engaged as animals respond to either conditioned or unconditioned aversive stimuli. Nevertheless, data from two previous studies suggest unique involvement of RMTg-projecting dmPFC neurons in the response to conditioned stimuli with inactivation of this projection significantly increasing cue-induced reinstatement of cocaine-seeking [47] and punished sucrose-seeking [48]. Future studies directly examining involvement of these cortical RMTg afferents in conditioned and unconditioned behavior will be crucial for delineating their involvement in various aspects of aversive signaling. Given that we observed a similar degree of input to the RMTg from both the PL and IL mPFC, it will also be interesting in future studies to determine whether input from these mPFC subregions exert similar or opposing actions on RMTg-mediated behavior. This could be especially interesting in light of previous studies suggesting that dorsal (e.g., PL) and ventral (e.g., IL) subregions of the mPFC exert opposing effects on many types of behavior [49, 50]. Our study also revealed a dense projection from the DP mPFC to the RMTg that exhibited a dramatic increase in density in the caudal mPFC. Unlike the PL and IL mPFC, very few studies have investigated the DP mPFC anatomically or functionally. In one of the few existing studies, Kataoka et al. [51] revealed a role for DP mPFC inputs to the dorsomedial hypothalamus in stress-induced avoidance of social interactions. These data further highlight the need for future work delineating the potentially unique roles that inputs to the RMTg from different cortical subregions play in mediating aversion.

Electrophysiological recordings in the present study showed that exposure to repeated foot shock resulted in a significant decrease in intrinsic excitability of RMTg-projecting dmPFC neurons. This contrasts with observations in LHb neurons, the densest source of input to the RMTg [2], which exhibit a significant increase in excitability following exposure to foot shock [52]. Interestingly, the decrease in excitability observed in the present study was accompanied by significant changes in the spine neck morphology of spines localized to the primary apical dendrites of RMTg-projecting dmPFC neurons. Dendritic spines are the main recipients of incoming excitatory signals in pyramidal neurons. Spine neck morphology plays a fundamental role in compartmentalizing electrical and biochemical signals in the head of the spine [53] and previous work found an inverse relationship between spine neck diameter and excitatory potential [54], Although speculative, the changes in spine neck morphology observed in the present study may be indicative of a reduction in the synaptic strength of inputs to RMTg-projecting dmPFC neurons in shock-exposed rats relative to controls. Keeping in mind the results from our cFos experiment that revealed significant recruitment of dmPFC-RMTg neuron activity following exposure to repeated foot shocks, these data suggest that RMTg-projecting dmPFC neurons undergo a compensatory response 24 hours after shock exposure that facilitates a loss of top-down control over RMTg-mediated activity. Such a loss could, upon re-exposure to the same stimulus, increase engagement of subcortical circuits to promote a more immediate and possibly stronger behavioral response. This may reflect sensitization or

reduced behavioral flexibility that could be adaptive in healthy contexts during which higher-order processes are not necessary for recall and appropriate responding to known aversive stimuli. Virally mediated approaches to measure circuit activity during behavioral testing could be used in future studies to test this intriguing hypothesis as well as delineate involvement of this circuit in conditioned versus unconditioned threat responding.

The results from the current study present a new perspective on the degree of subregion- and circuit-specific cortical regulation of RMTg-mediated aversive signaling. These observations provide a strong foundation for future studies that can investigate the distinct or complementary roles of parallel cortico-subcortical circuits involved in motivated behavior in both males and females. It will be of particular importance to determine whether the functional observations in the present study generalize to aversive stimuli of other sensory modalities. In addition, while much research has focused on RMTg-mediated inhibitory control over midbrain dopamine neurons, it is currently not known whether afferents from the dmPFC synapse onto VTA-projecting RMTg neurons to modulate dopamine release or RMTg neurons that project to other neuromodulatory nuclei (e.g., dorsal raphe, locus coeruleus). Finally, determining how these circuits are altered in models of neuropsychiatric illness will be crucial for understanding the neural mechanisms underlying disruptions in the balance of neural signals mediating reward and aversion that is altered in a number of disease states.

REFERENCES

1. Kaufling J, Veinante P, Pawlowski SA, Freund-Mercier M-J, Barrot M. Afferents to the GABAergic tail of the ventral tegmental area in the rat. J Comp Neurol. 2009;513:597–621.
2. Jhou TC, Geisler S, Marinelli M, Degarmo BA, Zahm DS. The mesopontine rostromedial tegmental nucleus: A structure targeted by the lateral habenula that projects to the ventral tegmental area of Tsai and substantia nigra compacta. J Comp Neurol. 2009;513:566–96.
3. Jhou TC, Fields HL, Baxter MG, Saper CB, Holland PC. The rostromedial tegmental nucleus (RMTg), a GABAergic afferent to midbrain dopamine neurons, encodes aversive stimuli and inhibits motor responses. Neuron. 2009;61:786–800.
4. Li H, Pullmann D, Cho JY, Eid M, Jhou TC. Generality and opponency of rostromedial tegmental (RMTg) roles in valence processing. ELife. 2019;8:e41542.
5. Elmer GI, Palacorolla H, Mayo CL, Brown PL, Jhou TC, Brady D, et al. The rostromedial tegmental nucleus modulates the development of stress-induced helpless behavior. Behav Brain Res. 2019;359:950–7.
6. Burgos-Robles A, Vidal-Gonzalez I, Quirk GJ. Sustained conditioned responses in prelimbic prefrontal neurons are correlated with fear expression and extinction failure. J Neurosci. 2009;29:8474–82.
7. Corcoran KA, Quirk GJ. Activity in prelimbic cortex is necessary for the expression of learned, but not innate, fears. J Neurosci. 2007;27:840–4.
8. Alexander WH, Brown JW. The role of the anterior cingulate cortex in prediction error and signaling surprise. Top Cogn Sci. 2019;11:119–35.
9. Hong S, Jhou TC, Smith M, Saleem KS, Hikosaka O. Negative reward signals from the lateral habenula to dopamine neurons are mediated by rostromedial tegmental nucleus in primates. J Neurosci. 2011;31:11457–71.
10. National Research Council. Guide for the care and use of laboratory animals. 8th ed. Washington DC: National Academies Press; 2011.
11. Stamatakis AM, Stuber GD. Activation of lateral habenula inputs to the ventral midbrain promotes behavioral avoidance. Nat Neurosci. 2012;24: https://doi.org/10.1038/nn.3145.
12. Wayman WN, Woodward JJ. Exposure to the abused inhalant toluene alters medial prefrontal cortex physiology. Neuropsychopharmacology. 2018;43:912–24.
13. McGuier NS, Padula AE, Lopez MF, Woodward JJ, Mulholland PJ. Withdrawal from chronic intermittent alcohol exposure increases dendritic spine density in the lateral orbitofrontal cortex of mice. Alcohol. 2015;49:21–27.
14. Gabbott PL, Dickie BG, Vaid RR, Headlam AJ, Bacon SJ. Local-circuit neurones in the medial prefrontal cortex (areas 25, 32 and 24b) in the rat: morphology and quantitative distribution. J Comp Neurol. 1997;377:465–99.
15. Lee AT, Vogt D, Rubenstein JL, Sohal VS. A class of GABAergic neurons in the prefrontal cortex sends long-range projections to the nucleus accumbens and elicits acute avoidance behavior. J Neurosci. 2014;34:11519–25.
16. Basu J, Zaremba JD, Cheung SK, Hitti FL, Zemelman BV, Losonczy A, et al. Gating of hippocampal activity, plasticity, and memory by entorhinal cortex long-range inhibition. Science. 2016;351:aaa5694.
17. Rock C, Zurita H, Lebby S, Wilson CJ, Apicella AJ. Cortical circuits of callosal GABAergic neurons. Cereb Cortex. 2018;28:1154–67.
18. Floresco SB. Prefrontal dopamine and behavioral flexibility: shifting from an 'inverted-U' toward a family of functions. Front Neurosci. 2013;7:62.
19. Vergara MD, Keller VN, Fuentealba JA, Gysling K. Activation of type 4 dopaminergic receptors in the prelimbic area of medial prefrontal cortex is necessary for the expression of innate fear behavior. Behav Brain Res. 2017;324:130–7.
20. Lauzon NM, Bechard M, Ahmad T, Laviolette SR. Supra-normal stimulation of dopamine D1 receptors in the prelimbic cortex blocks behavioral expression of both aversive and rewarding associative memories through a cyclic-AMP-dependent signaling pathway. Neuropharmacology. 2013;67:104–14.
21. Gonzalez MC, Kramar CP, Tomaiuolo M, Katche C, Weisstaub N, Cammarota M, et al. Medial prefrontal cortex dopamine controls the persistent storage of aversive memories. Front Behav Neurosci. 2014;8:408.
22. Castillo Díaz F, Kramar CP, Hernandez MA, Medina JH. Activation of D1/5 dopamine receptors in the dorsal medial prefrontal cortex promotes incubated-like aversive responses. Front Behav Neurosci. 2017;11:209.
23. Gaspar P, Bloch B, Le, Moine C. D1 and D2 receptor gene expression in the rat frontal cortex: cellular localization in different classes of efferent neurons. Eur J Neurosci. 1995;7:1050–63.
24. Mogil JS, Chesler EJ, Wilson SG, Juraska JM, Sternberg WF. Sex differences in thermal nociception and morphine antinociception in rodents depend on genotype. Neurosci Biobehav Rev. 2000;24:375–89.
25. Jolles JW, Boogert NJ, van den Bos R. Sex differences in risk-taking and associative learning in rats. R Soc Open Sci. 2015;2:150485.
26. Gruene TM, Flick K, Stefano A, Shea SD, Shansky RM. Sexually divergent expression of active and passive conditioned fear responses in rats. ELife. 2015;4:e11352.
27. Gabbott PLA, Warner TA, Jays PRL, Salway P, Busby SJ. Prefrontal cortex in the rat: projections to subcortical autonomic, motor, and limbic centers. J Comp Neurol. 2005;492:145–77.
28. Rozeske RR, Evans AK, Frank MG, Watkins LR, Lowry CA, Maier SF. Uncontrollable, but not controllable, stress desensitizes 5-HT1A receptors in the dorsal raphe nucleus. J Neurosci. 2011;31:14107–15.
29. Warden MR, Selimbeyoglu A, Mirzabekov JJ, Lo M, Thompson KR, Kim S-Y, et al. A prefrontal cortex-brainstem neuronal projection that controls response to behavioural challenge. Nature. 2012;492:428–32.
30. Bukalo O, Pinard CR, Silverstein S, Brehm C, Hartley ND, Whittle N, et al. Prefrontal inputs to the amygdala instruct fear extinction memory formation. Sci Adv. 2015;1:e1500251.
31. Economo MN, Clack NG, Lavis LD, Gerfen CR, Svoboda K, Myers EW, et al. A platform for brain-wide imaging and reconstruction of individual neurons. ELife. 2016;5:e10566.
32. Kebschull JM, Garcia da Silva P, Reid AP, Peikon ID, Albeanu DF, Zador AM. High-throughput mapping of single-neuron projections by sequencing of barcoded RNA. Neuron. 2016;91:975–87.
33. Mathis VP, Williams M, Fillinger C, Kenny PJ. Networks of habenula-projecting cortical neurons regulate cocaine seeking. Sci Adv. 2021;7:eabj2225.
34. Simmler LD, Ozawa T. Neural circuits in goal-directed and habitual behavior: implications for circuit dysfunction in obsessive-compulsive disorder. Neurochem Int. 2019;129:104464.
35. Loewke AC, Minerva AR, Nelson AB, Kreitzer AC, Gunaydin LA. Frontostriatal projections regulate innate avoidance behavior. J Neurosci. 2021;41:5487–501.
36. Rockland KS. Collateral branching of long-distance cortical projections in monkey. J Comp Neurol. 2013;521:4112–23.
37. Cruz AM, Kim TH, Smith RJ. Monosynaptic retrograde tracing from prelimbic neuron subpopulations projecting to either nucleus accumbens core or rostromedial tegmental nucleus. Front Neural Circuits. 2021;15:639733.
38. Santana N, Mengod G, Artigas F. Quantitative analysis of the expression of dopamine D1 and D2 receptors in pyramidal and GABAergic neurons of the rat prefrontal cortex. Cereb Cortex. 2009;19:849–60.
39. Vincent SL, Khan Y, Benes FM. Cellular colocalization of dopamine D1 and D2 receptors in rat medial prefrontal cortex. Synapse. 1995;19:112–20.
40. Vander Weele CM, Siciliano CA, Matthews GA, Namburi P, Izadmehr EM, Espinel IC, et al. Dopamine enhances signal-to-noise ratio in cortical-brainstem encoding of aversive stimuli. Nature. 2018;563:397–401.
41. Huang S, Zhang Z, Gambeta E, Xu SC, Thomas C, Godfrey N, et al. Dopamine inputs from the ventral tegmental area into the medial prefrontal cortex modulate neuropathic pain-associated behaviors in mice. Cell Rep. 2020;33:108393.
42. Floresco SB, Magyar O. Mesocortical dopamine modulation of executive functions: beyond working memory. Psychopharmacology. 2006;188:567–85.

43. Trantham-Davidson H, Burnett EJ, Gass JT, Lopez MF, Mulholland PJ, Centanni SW, et al. Chronic alcohol disrupts dopamine receptor activity and the cognitive function of the medial prefrontal cortex. J Neurosci. 2014;34:3706–18.

44. Trantham-Davidson H, Centanni SW, Garr SC, New NN, Mulholland PJ, Gass JT, et al. Binge-Like alcohol exposure during adolescence disrupts dopaminergic neurotransmission in the adult prelimbic cortex. Neuropsychopharmacology. 2017;42:1024–36.

45. Quiñones-Laracuente K, Vega-Medina A, Quirk GJ. Time-dependent recruitment of prelimbic prefrontal circuits for retrieval of fear memory. Front Behav Neurosci. 2021;15:665116.

46. Li H, Pullmann D, Jhou TC. Valence-encoding in the lateral habenula arises from the entopeduncular region. ELife. 2019;8:e41223.

47. Cruz AM, Spencer HF, Kim TH, Jhou TC, Smith RJ. Prelimbic cortical projections to rostromedial tegmental nucleus play a suppressive role in cue-induced reinstatement of cocaine seeking. Neuropsychopharmacology. 2020. https://doi.org/10.1038/s41386-020-00909-z.

48. Li H, Vento PJ, Parrilla-Carrero J, Pullmann D, Chao YS, Eid M, et al. Three rostromedial tegmental afferents drive triply dissociable aspects of punishment learning and aversive valence encoding. Neuron. 2019;17. https://doi.org/10.1016/j.neuron.2019.08.040.

49. Peters J, Kalivas PW, Quirk GJ. Extinction circuits for fear and addiction overlap in prefrontal cortex. Learn Mem. 2009;16:279–88.

50. Gourley SL, Taylor JR. Going and stopping: dichotomies in behavioral control by the prefrontal cortex. Nat Neurosci. 2016;19:656–64.

51. Kataoka N, Shima Y, Nakajima K, Nakamura K. A central master driver of psychosocial stress responses in the rat. Science. 2020;367:1105–12.

52. Lecca S, Pelosi A, Tchenio A, Moutkine I, Lujan R, Hervé D, et al. Rescue of GABAB and GIRK function in the lateral habenula by protein phosphatase 2A inhibition ameliorates depression-like phenotypes in mice. Nat Med. 2016;22:254–61.

53. Tønnesen J, Katona G, Rózsa B, Nägerl UV. Spine neck plasticity regulates compartmentalization of synapses. Nat Neurosci. 2014;17:678–85.

54. Araya R, Vogels TP, Yuste R. Activity-dependent dendritic spine neck changes are correlated with synaptic strength. Proc Natl Acad Sci USA. 2014;111:E2895–2904.

AUTHOR CONTRIBUTIONS
EJG and LJC conceived of and designed experiments. EJG and EMS collected and analyzed data for in-vivo optogenetics experiments. EJG, EMS, and AG collected and analyzed data for tract tracing experiments. EJG, EMS, and CLA collected and analyzed data for collaterals experiment. EJG, EMS, and KCS collected and analyzed data for dendritic spine analysis. EJG, AHS, DTV, and LJC collected and analyzed data for in-situ hybridization experiments. EJG, WNW, JJW collected and analyzed data for ex-vivo slice electrophysiology experiments. EJG, JJW, and LJC contributed to interpretation of findings. EJG and LJC drafted the manuscript with WNW and JJW providing critical revisions. All authors reviewed manuscript content and approved of the final version prior to publication.

COMPETING INTERESTS
The authors declare no competing interests.

ADDITIONAL INFORMATION
Supplementary information The online version contains supplementary material available at https://doi.org/10.1038/s41386-023-01612-5.

Correspondence and requests for materials should be addressed to Elizabeth J. Glover.

Reprints and permission information is available at http://www.nature.com/reprints

Publisher's note Springer Nature remains neutral with regard to jurisdictional claims in published maps and institutional affiliations.